Interacting spin waves in the ferromagnetic Kondo lattice model

A. Schwabe[1,2,*] and W. Nolting[1]
[1]*Festkörpertheorie, Institut für Physik, Humboldt-Universität, 12489 Berlin, Germany*
[2]*I. Institut für Theoretische Physik, Universität Hamburg, 20355 Hamburg, Germany*

(Received 31 July 2009; revised manuscript received 27 October 2009; published 9 December 2009; corrected 14 December 2009)

We present an approach for the ferromagnetic, three-dimensional, and translational-symmetric Kondo lattice model, which allows us to derive both magnon energies and linewidths (lifetimes) and to study the properties of the ferromagnetic phase at finite temperatures. Both "anomalous softening" and "anomalous damping" are obtained and discussed. Our method consists of mapping the Kondo lattice model onto an effective Heisenberg model by means of the "modified RKKY interaction" and the "interpolating self-energy approach." The Heisenberg model is approximately solved by applying the Dyson-Maleev transformation and using the "spectral density approach" with a broadened magnon spectral density.

DOI: 10.1103/PhysRevB.80.214408 PACS number(s): 75.30.Mb, 75.50.Pp, 75.30.Ds, 75.10.Jm

I. INTRODUCTION

The Kondo lattice model[1] describes the interaction between two groups of electrons. One group consists of itinerant conduction-band electrons, which can hop to different lattice sites. The other group concerns localized electrons that couple to a magnetic moment of spin S localized at a certain lattice site. Both subsystems can perform an intraatomic interaction with each other while neglecting interactions between the itinerant electrons or between the localized spins. For nondegenerated band electrons in real space, the Hamiltonian reads as

$$H = \sum_{ij\sigma} T_{ij} c_{i\sigma}^{\dagger} c_{j\sigma} - \frac{J}{2} \sum_{i\sigma} (z_{\sigma} S_i^z c_{i\sigma}^{\dagger} c_{i\sigma} + S_i^{-\sigma} c_{i\sigma}^{\dagger} c_{i-\sigma}), \quad \text{(1a)}$$

$$z_{\sigma} = \delta_{\sigma\uparrow} - \delta_{\sigma\downarrow}, \quad S^{\sigma} = S^{+}\delta_{\sigma\uparrow} + S^{-}\delta_{\sigma\downarrow}, \quad \text{(1b)}$$

where $c_{i\sigma}^{(\dagger)}$ represents an annihilation (creation) operator for an electron of spin projection σ at a lattice site $\mathbf{R}_i$. J is the Hund's coupling constant and T_{ij} are the hopping integrals. Since we are investigating the ferromagnetic Kondo lattice model, $J>0$.

The second term in Eq. (1a) describes an Ising-like interaction between the z components of the localized and the itinerant spin. The third term accounts for the spin-exchange processes between the two subsystems. We will treat the three-dimensional, translational-symmetric, and infinitely extended Kondo lattice model.

The Kondo lattice model is believed to characterize the basic physics of a wide variety of solid-state materials.

Magnetic semiconductors, e.g., EuO, are a prominent class of substances, which draw notable attention due to the "redshift" of the optical-absorption edge upon cooling from $T=T_C$ to $T=0$K. One can conclude that the coupling constant J is positive and of the order of some tenth of eV. In contrast, the magnetic ordering of the localized spins is explained via special superexchange mechanisms.

Ferromagnetic local-moment metals, such as Gd, are another application. An RKKY-(Ruderman and Kittel,[2] Kasuya,[3] Yosida[4]) type interaction is supposed to create the ferromagnetic order. The magnetism relies on localized $4f$ electrons that are shielded from the $4f$ orbitals of adjacent atoms by other completely filled orbitals. On the other side, the conductivity properties are determined by itinerant $5d$ or $6s$ electrons.

The discovery of the "colossal magnetoresistance" and its promising technological application motivated a considerable research effort that is related to the manganese oxides with perovskite structures $T_{1-x}D_xMnO_3$ (T=La, Pr, Nd; D=Sr, Ca, Ba, Pb). A prototype is the well-known compound $La_{1-x}Ca_xMnO_3$, which can be obtained by replacing a trivalent La^{3+} ion with the divalent earth-alkali ion Ca^{2+} in $La^{3+}Mn^{3+}O_3$, leading to a homogeneous valence mixture of the manganese ions $Mn^{3+}_{1-x}Mn^{4+}_x$. The three $3d$-t_{2g} electrons of Mn^{4+} are considered as localized forming a spin of $S=\frac{3}{2}$. They are coupled to the $n=(1-x)$ itinerant $3d$-e_g electrons per Mn site by a ferromagnetic coupling $J>0$. J is estimated to be much larger than the electronic bandwidth since the manganites are bad electrical conductors.

Many fascinating features of the Kondo lattice model can be accredited to the complex correlation between the magnetic and electronic subsystem. In this regard, one challenging issue represents the "anomalous softening" of the spin-wave dispersion, which has attracted comprehensive interest. The spin-wave dispersion relation of manganites with high-T_C resembles one of a simple Heisenberg model with nearest-neighbor exchange only.[5,6] However, some manganites with lower-T_C exhibit apparent deviations from this behavior that are strongly dependent on the band occupation.[6–9] Despite extensive theoretical work in this field, the softening of the dispersion relation near the boundaries of the Brillouin zone still lacks a complete explanation. Currently, disorder-induced softening has been excluded for some materials.[6,8] On the other hand, the incorporation of an antiferromagnetic superexchange interaction between the Mn ions into the Hamiltonian of the Kondo lattice model has been proposed to take into account the antiferromagnetic tendencies of the parent material $LaMnO_3$.[10]

In recent years, unusually large magnon damping at the Brillouin-zone boundaries and low temperatures has come to the fore. This is frequently referred to as "anomalous damping."[6,7] Evidence has been found in neutron-scattering experiments with manganites and raised questions concerning the nature of anomalous damping and its link to anoma-

lous softening. Besides the electron-magnon interaction, some authors speculate about a magnon-phonon coupling for certain manganites as an origin,[7] while other authors reject it.[9] Thus, it is of crucial importance to develop reliable spin-wave theories for the Kondo lattice model and to study whether anomalous damping can be traced back to the electron-magnon interaction.

In this work, we concentrate on the magnetic subsystem of the Kondo lattice model. The aim is to investigate the dependencies of the energy as well as the linewidths of the elementary magnetic excitations called spin waves or magnons, respectively. A subsection of the paper will treat the anomalous features of the magnon spectrum mentioned above and include a discussion of the influence of temperature.

We will present a solution for the Kondo lattice model, which is as well applicable to the Heisenberg model. It goes explicitly beyond standard methods, such as the "random-phase approximation," by accounting for correlations of higher order. Although nonpertubative, it is still controlled in the sense that, in principle, it results from the moments of an exact high-energy expansion. We assume quantum spins, so our theory is not restricted to the classical limit of large spin values $S \gg 1$.

The paper is structured as follows. First, we will demonstrate how the Kondo lattice model is mapped onto a Heisenberg model (Sec. II). Both employed theories, the "modified RKKY interaction" and the "interpolating self-energy approach," have been already successfully applied to the Kondo lattice model for various other problems.[11–15] They will fix the electron-spin interaction. In Sec. III, we will focus on the spin-spin interaction by presenting a solution for the Heisenberg model that will not only allow us to calculate the energy of the magnetic excitations but also their linewidth. Section IV will proceed with numerical results for the Kondo lattice model that provide insights into the properties of its ferromagnetic phase and an investigation of the dependence on the intra-atomic coupling constant J, the conduction-band occupation n, and the temperature T.

II. MAPPING ONTO A HEISENBERG MODEL

The Kondo lattice model provokes a complex many-body problem solvable only in a few limiting cases. Hence, we try mapping the Hamiltonian of the Kondo lattice model (1a) onto an effective Heisenberg Hamiltonian, in which the conduction-band electrons mediate the indirect exchange interaction between the localized spins. The idea is to use the "modified RKKY interaction[13,16]" (mRKKY), wherein the Hamiltonian is averaged in the electronic subspace

$$H_{\mathrm{s}} = -\frac{J}{2}\sum_{i\sigma}\left(z_\sigma S_i^z \langle c_{i\sigma}^\dagger c_{i\sigma}\rangle^{(\mathrm{s})} + S_i^{-\sigma}\langle c_{i\sigma}^\dagger c_{i-\sigma}\rangle^{(\mathrm{s})}\right). \tag{2}$$

The arising expectation value $\langle c_{i\sigma}^\dagger c_{i-\sigma}\rangle^{(\mathrm{s})}$ does not vanish generally since the spin conservation is valid for the total system of the localized spins and the itinerant electrons while the averaging is done in the electronic subspace only. The expectation values can be calculated by using the spectral theorem and the corresponding electron Green's functions called "restricted Green's functions"

$$\langle c_{i\sigma}^\dagger c_{i\sigma}\rangle^{(\mathrm{s})} = -\frac{1}{\pi\hbar}\int dE f_-(E)\,\mathrm{Im}\, G_{ii}^{\sigma\sigma,(\mathrm{s})}, \tag{3a}$$

$$G_{ij}^{\sigma\sigma,(\mathrm{s})} = \langle\langle c_{i\sigma}; c_{j\sigma}^\dagger\rangle\rangle^{(\mathrm{s})}, \tag{3b}$$

$$\langle c_{i\sigma}^\dagger c_{i-\sigma}\rangle^{(\mathrm{s})} = -\frac{1}{\pi\hbar}\int dE f_-(E)\,\mathrm{Im}\, G_{ii}^{-\sigma\sigma,(\mathrm{s})}, \tag{4a}$$

$$G_{ij}^{-\sigma\sigma,(\mathrm{s})} = \langle\langle c_{i-\sigma}; c_{j\sigma}^\dagger\rangle\rangle^{(\mathrm{s})}, \tag{4b}$$

where $f_-(E)$ is the Fermi function. After introducing the free Green's function for noninteracting electrons $G_{ij}^{(0)}(E)$, the equations of motion of $G_{ij}^{\sigma\sigma,(\mathrm{s})}(E)$ and $G_{ij}^{-\sigma\sigma,(\mathrm{s})}(E)$ can be solved

$$G_{ij}^{\sigma\sigma,(\mathrm{s})}(E) = G_{ij}^{(0)}(E) - \frac{J}{2}\sum_l G_{il}^{(0)}\left(z_\sigma S_l^z \langle\langle c_{l\sigma}; c_{j\sigma}^\dagger\rangle\rangle^{(\mathrm{s})} + S_l^{-\sigma}\langle\langle c_{l-\sigma}; c_{j\sigma}^\dagger\rangle\rangle^{(\mathrm{s})}\right), \tag{5}$$

$$G_{ij}^{-\sigma\sigma,(\mathrm{s})}(E) = -\frac{J}{2}\sum_l G_{il}^{(0)}\left(-z_\sigma S_l^z \langle\langle c_{l-\sigma}; c_{j\sigma}^\dagger\rangle\rangle^{(\mathrm{s})} + S_l^{\sigma}\langle\langle c_{l\sigma}; c_{j\sigma}^\dagger\rangle\rangle^{(\mathrm{s})}\right). \tag{6}$$

Now we replace the restricted Green's functions on the right-hand sides of Eqs. (5) and (6) with their full equivalents

$$G_{ij}^{\sigma\sigma,(\mathrm{s})}(E) \to G_{ij\sigma}(E) = \langle\langle c_{i\sigma}; c_{j\sigma}^\dagger\rangle\rangle, \tag{7}$$

$$G_{ij}^{-\sigma\sigma,(\mathrm{s})}(E) \to G_{ij}^{-\sigma\sigma}(E) = 0. \tag{8}$$

$G_{ij}^{-\sigma\sigma}(E)$ vanishes because of spin conservation. $G_{ij\sigma}(E)$ labels the Green's function of interacting electrons.

These solutions are inserted into the averaged Hamiltonian (2). Eventually, our approach leads to an effective Heisenberg Hamiltonian[17]

$$H_{\mathrm{Kondo}} \overset{\mathrm{mRKKY}}{\to} H_{\mathrm{eff}} = -\sum_{ij} J_{ij}\mathbf{S}_i\cdot\mathbf{S}_j. \tag{9}$$

The effective exchange integrals are functionals of the electronic self-energy $\Sigma_{ij\sigma}(E)$ via the electron Green's function $G_{ij\sigma}(E)$,

$$J_{ij} = \frac{J^2}{4\pi\hbar^2}\int dE f_-(E)\,\mathrm{Im}\sum_\sigma G_{ij}^{(0)}(E)G_{ij\sigma}(E). \tag{10}$$

The replacements (5) and (6) comprise many-body correlations of higher order than the conventional RKKY theory that would be obtained by replacing

$$G_{ij}^{\sigma\sigma,(\mathrm{s})}(E) \to G_{ij}^{(0)}(E), \quad G_{ij}^{-\sigma\sigma,(\mathrm{s})}(E) \to 0. \tag{11}$$

We use the interpolating self-energy approach[18] (ISA) in order to set the electronic self-energy $\Sigma_{ij\sigma}(E)$. It is derived for the limiting cases of the ferromagnetically ordered semiconductor, the atomic limit, and second-order pertubation theory assuming vanishing band occupation $n = \Sigma_\sigma \langle c_{i\sigma}^\dagger c_{i\sigma}\rangle \to 0$. An

interpolation between the limiting cases performed by fitting leading terms in its rigorous high-energy expansion provides the result

$$\Sigma_{ij\sigma}(E) = -\frac{J}{2}z_\sigma\langle S^z\rangle\delta_{ij} + \frac{J^2}{4}\frac{a_\sigma G_{ii}^{(0)}\left(E-\frac{1}{2}Jz_\sigma\langle S^z\rangle\right)}{1-b_\sigma G_{ii}^{(0)}\left(E-\frac{1}{2}Jz_\sigma\langle S^z\rangle\right)}\delta_{ij}, \tag{12a}$$

$$a_\sigma = S(S+1) - z_\sigma\langle S^z\rangle(z_\sigma\langle S^z\rangle + 1), \quad b_\sigma = \frac{J}{2}. \tag{12b}$$

Although derived in the low-concentration limit, we apply the self-energy (12a) to the case of finite band occupations $n>0$.

In summary, the problem is reduced to the solution of an effective Heisenberg model with exchange integrals J_{ij} that depend on the coupling constant J, the band occupation n, and the temperature T: $J_{ij}=J_{ij}(J,n,T)$.

III. EFFECTIVE HEISENBERG MODEL

A. Solution

It is convenient to transform the spin operators $\mathbf{S}_i$ of the effective Heisenberg Hamiltonian (9) into bosonic magnon operators $\{a_i, a_i^\dagger, n_i=a_i^\dagger a_i\}$ by means of the Dyson-Maleev transformation[19–21]

$$S_i^+ = \sqrt{2S}a_i, \quad S_i^- = \sqrt{2S}a_i^\dagger\left(1-\frac{n_i}{2S}\right), \tag{13a}$$

$$S_i^z = S - n_i. \tag{13b}$$

After a Fourier transformation, the Heisenberg Hamiltonian then reads in momentum space as

$$H_{\text{Heisenberg}} \to H_{\text{DM}} = \frac{1}{N}\sum_{\mathbf{q}'}\hbar\omega_{\mathbf{q}'}n_{\mathbf{q}'} + \frac{1}{N^4}\sum_{\mathbf{q}_1\cdots\mathbf{q}_4}(J_{\mathbf{q}_4}-J_{\mathbf{q}_1-\mathbf{q}_3})a_{\mathbf{q}_1}^\dagger a_{\mathbf{q}_2}^\dagger a_{\mathbf{q}_3}a_{\mathbf{q}_4}\delta_{\mathbf{q}_1+\mathbf{q}_2,\mathbf{q}_3+\mathbf{q}_4}, \tag{14}$$

where $\hbar\omega_{\mathbf{q}}=2S(J_0-J_{\mathbf{q}})$ stands for the bare energy of a free magnon with momentum $\mathbf{q}$ and N for the number of lattice sites. The second summand of H_{DM} in Eq. (14) describes the magnon-magnon interaction and causes the existence of finite linewidths and the renormalization of the magnon energy. The Dyson-Maleev transformation makes it possible to take the complete interaction between the magnons into account without making approximations that are necessary for other theories, e.g., the Holstein-Primakoff transformation.[22]

At this stage, we need to mention that the transformation (13a) and (13b) leads to unphysical states for temperatures near the transition temperature T_C since we transform from a Hilbert space, which is $(2S+1)$ dimensional into one with infinite dimensions. Nevertheless, according to Dyson, the contributions to the free energy from these unphysical states are smaller than $\exp(-\alpha\frac{T_C}{T})$, where α is a coefficient of order unity.[20]

Additionally, S_i^+ and S_i^- are not Hermitian conjugated in the Dyson-Maleev formalism. However, Bar'yakhtar *et al.*[23] showed that the contributions to spin-correlation functions from unphysical states, arising from the non-Hermiticity, are of the order of $\exp(-\frac{T^*}{T})$, where $k_BT^*=S(2S+1)J_0$.

The bosonic Heisenberg model (14) is solved by applying the "spectral density approach." The spectral moments of the spectral density $S_{\mathbf{q}}(E)$ are defined by

$$M_{\mathbf{q}}^{(n)} = \frac{1}{\hbar}\int dE E^n S_{\mathbf{q}}(E), \tag{15}$$

but they can also be evaluated exactly and independently from Eq. (15) by the following relation:

$$M_{\mathbf{q}}^{(n)} = \langle[\underbrace{[[a_{\mathbf{q}},H]_-,\ldots,H]_-}_{p\text{-fold commutator}},\underbrace{[H,\ldots,[H,a_{\mathbf{q}}^\dagger]_-]_-}_{(n-p)\text{-fold commutator}}]_-\rangle. \tag{16}$$

The approach requires a spectral density, which is usually guessed, e.g., from experiments or theoretical considerations. Parameters of $S_{\mathbf{q}}(E)$ can be evaluated by a sufficient set of equations that is derived from the equivalence of Eqs. (15) and (16).

In our case, $S_{\mathbf{q}}(E)$ represents the magnon spectral density, which is associated with the average magnon occupation number by the spectral theorem

$$\langle a_{\mathbf{q}}^\dagger a_{\mathbf{q}}\rangle = \langle n_{\mathbf{q}}\rangle = \frac{1}{\hbar}\int dE f_+(E)S_{\mathbf{q}}(E), \tag{17}$$

where $f_+(E)$ is the Bose function. Since we are interested in lifetime effects, we need to fit the first three spectral moments $M_{\mathbf{q}}^{(n\le 2)}$ and use a spectral density of finite width. The renormalized magnon energies $\hbar\Omega_{\mathbf{q}}$ and their spectral linewidths $\Gamma_{\mathbf{q}}$ or lifetimes, respectively,

$$\tau_{\mathbf{q}} = \frac{\hbar}{\Gamma_{\mathbf{q}}} \tag{18}$$

work as parameters that need to be calculated from the set of equations.

For simplicity and without loss of generality, we want to restrict our derivation to a symmetric spectral density $S_{\mathbf{q}}(\hbar\Omega_{\mathbf{q}}+E)=S_{\mathbf{q}}(\hbar\Omega_{\mathbf{q}}-E)$.[24] This is in agreement with neutron-scattering experiments[25] and other theories,[26] where $S_{\mathbf{q}}(E)$ has the approximate shape of a Lorentzian

$$S_{\mathbf{q}}^{\text{Lorentzian}}(E) = \frac{\hbar\Gamma_{\mathbf{q}}}{\pi}\frac{1}{(E-\hbar\Omega_{\mathbf{q}})^2+\Gamma_{\mathbf{q}}^2} \tag{19}$$

or a Gaussian, respectively,

$$S_{\mathbf{q}}^{\text{Gaussian}}(E) = \frac{\hbar}{\sqrt{\pi}\Gamma_{\mathbf{q}}}e^{-(E-\hbar\Omega_{\mathbf{q}}/\Gamma_{\mathbf{q}})^2}. \tag{20}$$

One must keep in mind that the Lorentzian must be restricted to a finite energy interval, ensuring a finite second spectral moment $M_{\mathbf{q}}^{(2)}$.

The zeroth spectral moment

$$M_{\mathbf{q}}^{(0)} = \langle [a_{\mathbf{q}}, a_{\mathbf{q}}^{\dagger}]_- \rangle = 1 \tag{21}$$

expects a normalized spectral density $S_{\mathbf{q}}(E)$ according to Eq. (15). For the first spectral moment, we get

$$\begin{aligned} M_{\mathbf{q}}^{(1)} &= \langle [[a_{\mathbf{q}}, H_{\mathrm{DM}}]_-, a_{\mathbf{q}}^{\dagger}]_- \rangle \\ &= \hbar\omega_{\mathbf{q}} M_{\mathbf{q}}^{(0)} + \frac{2}{N}\sum_{\mathbf{q}'} (J_{\mathbf{q}} + J_{\mathbf{q}'} - J_0 - J_{\mathbf{q}'-\mathbf{q}}) \langle n_{\mathbf{q}'} \rangle . \end{aligned} \tag{22}$$

The result for the second spectral moment is

$$\begin{aligned} M_{\mathbf{q}}^{(2)} &= \langle [[[a_{\mathbf{q}}, H_{\mathrm{DM}}]_-, [H_{\mathrm{DM}}, a_{\mathbf{q}}^{\dagger}]_-]_- \rangle \\ &= 2\hbar\omega_{\mathbf{q}} M_{\mathbf{q}}^{(1)} - (\hbar\omega_{\mathbf{q}} M_{\mathbf{q}}^{(0)})^2 \\ &\quad + \frac{1}{N^4} \sum_{\mathbf{q}_1 \cdots \mathbf{q}_4} (J_{\mathbf{q}_3} + J_{\mathbf{q}_4} - J_{\mathbf{q}_3-\mathbf{q}} - J_{\mathbf{q}_4-\mathbf{q}}) \\ &\quad \times (J_{\mathbf{q}} + J_{\mathbf{q}_1+\mathbf{q}_2-\mathbf{q}} - J_{\mathbf{q}_1-\mathbf{q}} - J_{\mathbf{q}_2-\mathbf{q}}) \\ &\quad \times (2\langle a_{\mathbf{q}_3+\mathbf{q}_4-\mathbf{q}}^{\dagger} a_{\mathbf{q}_3} a_{\mathbf{q}_2}^{\dagger} a_{\mathbf{q}_1+\mathbf{q}_2-\mathbf{q}} \rangle \delta_{\mathbf{q}_1,\mathbf{q}_4} \\ &\quad + 2\langle a_{\mathbf{q}_3+\mathbf{q}_4-\mathbf{q}}^{\dagger} a_{\mathbf{q}_2}^{\dagger} a_{\mathbf{q}_3} a_{\mathbf{q}_1+\mathbf{q}_2-\mathbf{q}} \rangle \delta_{\mathbf{q}_1,\mathbf{q}_4} \\ &\quad - \langle a_{\mathbf{q}_1}^{\dagger} a_{\mathbf{q}_2}^{\dagger} a_{\mathbf{q}_3} a_{\mathbf{q}_4} \rangle \delta_{\mathbf{q}_1+\mathbf{q}_2,\mathbf{q}_3+\mathbf{q}_4}) . \end{aligned} \tag{23}$$

A simple ansatz for the unknown higher expectation values in Eq. (23), such as $\langle a_{\mathbf{q}_3+\mathbf{q}_4-\mathbf{q}}^{\dagger} a_{\mathbf{q}_3} a_{\mathbf{q}_2}^{\dagger} a_{\mathbf{q}_1+\mathbf{q}_2-\mathbf{q}} \rangle$, is derived by decoupling them using a mean-field approximation with respect to the momentum conservation,

$$\begin{aligned} &\langle a_{\mathbf{q}_3+\mathbf{q}_4-\mathbf{q}}^{\dagger} a_{\mathbf{q}_3} a_{\mathbf{q}_2}^{\dagger} a_{\mathbf{q}_1+\mathbf{q}_2-\mathbf{q}} \rangle \delta_{\mathbf{q}_1,\mathbf{q}_4} \\ &\quad \overset{MF}{\rightarrow} \langle a_{\mathbf{q}_3+\mathbf{q}_4-\mathbf{q}}^{\dagger} a_{\mathbf{q}_3} \rangle \langle a_{\mathbf{q}_2}^{\dagger} a_{\mathbf{q}_1+\mathbf{q}_2-\mathbf{q}} \rangle \delta_{\mathbf{q}_1,\mathbf{q}_4} \delta_{\mathbf{q}_4,\mathbf{q}} \\ &\qquad + \langle a_{\mathbf{q}_3+\mathbf{q}_4-\mathbf{q}}^{\dagger} a_{\mathbf{q}_1+\mathbf{q}_2-\mathbf{q}} \rangle \langle a_{\mathbf{q}_2}^{\dagger} a_{\mathbf{q}_3} \rangle \delta_{\mathbf{q}_1,\mathbf{q}_4} \delta_{\mathbf{q}_2,\mathbf{q}_3} \\ &\quad \ldots . \end{aligned} \tag{24}$$

Therewith, the solution is formally completed

$$\begin{aligned} M_{\mathbf{q}}^{(2)} &= (\hbar\omega_{\mathbf{q}} M_{\mathbf{q}}^{(0)})^2 \\ &\quad + \frac{1}{N^2} \sum_{\mathbf{q}'} \sum_{\mathbf{q}''} [2(J_{\mathbf{q}'} + J_{\mathbf{q}''-\mathbf{q}'+\mathbf{q}} - J_{\mathbf{q}'-\mathbf{q}} - J_{\mathbf{q}''-\mathbf{q}'}) \\ &\quad \times (J_{\mathbf{q}} + J_{\mathbf{q}''} - J_{\mathbf{q}'-\mathbf{q}} - J_{\mathbf{q}''-\mathbf{q}'}) \\ &\quad - (J_{\mathbf{q}'} + J_{\mathbf{q}''} - J_{\mathbf{q}'-\mathbf{q}} - J_{\mathbf{q}''-\mathbf{q}}) \\ &\quad \times (J_{\mathbf{q}} + J_{\mathbf{q}'+\mathbf{q}''-\mathbf{q}} - J_{\mathbf{q}'-\mathbf{q}} - J_{\mathbf{q}''-\mathbf{q}})] \langle n_{\mathbf{q}'} \rangle \langle n_{\mathbf{q}''} \rangle . \end{aligned} \tag{25}$$

For numerical reasons, we still need to simplify Eq. (25) to prevent eight-dimensional integrals in expressions, such as $\frac{1}{N^2}\Sigma_{\mathbf{q}'}\Sigma_{\mathbf{q}''} J_{\mathbf{q}''-\mathbf{q}'+\mathbf{q}} J_{\mathbf{q}''} \langle n_{\mathbf{q}'} \rangle \langle n_{\mathbf{q}''} \rangle$. This is done by exploiting the translational symmetry

$$J_0 - J_{\mathbf{q}} = \sum_{\text{shells } i} z_i J_i (1 - \gamma_{\mathbf{q}}^{(i)}), \tag{26a}$$

$$\gamma_{\mathbf{q}}^{(i)} = \frac{1}{z_i} \sum_{\substack{\mathbf{R} \text{ of} \\ \text{shell } i}} e^{i\mathbf{q}\cdot\mathbf{R}} . \tag{26b}$$

A shell is defined by all lattice sites $\mathbf{R}$ at the same distance $|\mathbf{R} - \tilde{\mathbf{R}}|$ to an offset lattice site $\tilde{\mathbf{R}}$.[27] Thereby, z_i denotes the number of all lattice sites of shell i and J_i the exchange integral of shell i. The shells are numbered and sorted by the size of their radii, i.e., $i=1$ stands for the nearest neighbors, $i=2$ for the next-nearest neighbors, etc. Within the shell concept, the problematic terms easily factorize[28]

$$\begin{aligned} &\frac{1}{N^2} \sum_{\mathbf{q}'\mathbf{q}''} \gamma_{\mathbf{q}''-\mathbf{q}'-\mathbf{q}_1}^{(i)} \gamma_{\mathbf{q}''-\mathbf{q}_2}^{(j)} \langle n_{\mathbf{q}'} \rangle \langle n_{\mathbf{q}''} \rangle \\ &\quad = \gamma_{\mathbf{q}_1}^{(i)} \gamma_{\mathbf{q}_2}^{(j)} \frac{1}{N} \sum_{\mathbf{q}'} (\gamma_{\mathbf{q}'}^{(i)} \langle n_{\mathbf{q}'} \rangle) \sum_{\text{shells } m} N_{ijm} \frac{1}{N} \sum_{\mathbf{q}''} \gamma_{\mathbf{q}''}^{(m)} \langle n_{\mathbf{q}''} \rangle , \end{aligned} \tag{27}$$

where we use a notation similar to Dvey-Aharon and Fibich[29]

$$N_{ijm} = \frac{1}{z_i z_j} \sum_{\mathbf{R}_i, \mathbf{R}_j} \delta_{\mathbf{R}_i + \mathbf{R}_j, \mathbf{R}_m} . \tag{28}$$

N_{ijm} gives the number of shell vectors $\mathbf{R}_m$ that can be constructed out of the sum of shell vectors of the shells i and j

$$\mathbf{R}_i + \mathbf{R}_j = \mathbf{R}_m . \tag{29}$$

By applying the shell concept not only to the expressions of the second spectral moment $M_{\mathbf{q}}^{(2)}$ in Eq. (25) but also to the first spectral moment $M_{\mathbf{q}}^{(1)}$ in Eq. (22), we finally obtain after some algebra

$$\hbar\Omega_{\mathbf{q}} = 2 \sum_{\text{shells } i} z_i J_i (1 - \gamma_{\mathbf{q}}^{(i)})(S - A_i), \tag{30a}$$

$$\Gamma_{\mathbf{q}}^2 \tilde{m}_{\mathbf{q}} = 4 \sum_{\text{shells } i,j} z_i z_j J_i J_j F_{ij} \cdot (1 - \gamma_{\mathbf{q}}^{(i)})[F_{ij} + (A_j - A_i)(1 - \gamma_{\mathbf{q}}^{(j)})] . \tag{30b}$$

The influence of the shape of $S_{\mathbf{q}}(E)$ on the second spectral moment $M_{\mathbf{q}}^{(2)}$ is contained in the dimensionless quantity $\tilde{m}_{\mathbf{q}}$

$$\tilde{m}_{\mathbf{q}} = \frac{1}{\hbar} \int dx x^2 \Gamma_{\mathbf{q}} S_{\mathbf{q}}(x\Gamma_{\mathbf{q}} + \hbar\Omega_{\mathbf{q}}) . \tag{31}$$

When using a Lorentzian or a Gaussian spectral density, $\tilde{m}_{\mathbf{q}}$ is advantageously independent in the momentum $\mathbf{q}$.

F_{ij} is merely determined by the A_i

$$F_{ij} = A_0 - A_i - N_{ij0} A_0 - \sum_{\text{shells } m>0} N_{ijm} (A_0 - A_m) . \tag{32}$$

Therewith, the A_i remain the only unknown quantities in Eq. (30a) and (30b) at a given temperature. Because of the definition

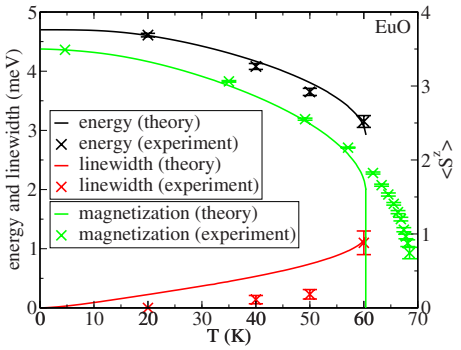

FIG. 1. (Color online) Temperature dependence of the magnon energy $\hbar\Omega_q(T)$ and the linewidth $\Gamma_q(T)$ for $q=|\mathbf{q}|=0.8$ Å^{-1} and of the magnetization $\langle S^z\rangle(T)$. The calculations (lines) are carried out for the parameters of EuO (Ref. 30) in comparison to experimental data from Refs. 25, 31, and 32 (crosses). As in the experimental analysis, a Lorentzian (19) is used for the magnon spectral density $S_{\mathbf{q}}(E)$.

$$A_i = \begin{cases} \dfrac{1}{N}\displaystyle\sum_{\mathbf{q}'} \langle n_{\mathbf{q}'}\rangle & \text{if } i=0 \\ \dfrac{1}{N}\displaystyle\sum_{\mathbf{q}'} (1-\gamma_{\mathbf{q}'}^{(i)})\langle n_{\mathbf{q}'}\rangle & \text{if } i>0, \end{cases} \tag{33}$$

the A_i depend on the spectral density $S_{\mathbf{q}}(E)$ and via the Eqs. (30a) and (30b) on each other

$$A_i = A_i(\{A_j\}). \tag{34}$$

Therefore, they have to be self-consistently calculated. With the solution satisfying Eq. (34), one can directly compute $\hbar\Omega_{\mathbf{q}}$ and $\Gamma_{\mathbf{q}}$ for a given momentum $\mathbf{q}$.

B. Comparison to experimental data and other theories

In terms of checking our theory for a real system, we consider the Heisenberg ferromagnet EuO, whose exchange integrals J_1 and J_2 are known.[30] According to Fig. 1, a good agreement concerning the magnon properties $\hbar\Omega_{\mathbf{q}}$ and $\Gamma_{\mathbf{q}}$, and the magnetization $\langle S^z\rangle$ can be found between the numerical results of our theory and the experimental data for a wide range of low and intermediate temperatures and for not-too-small momenta.[25,30–32] At temperatures near T_C, the unphysical states cause a wrong first-order phase transition that contradicts the experimental data.

Results similar to Eq. (30b) have been obtained by other theories of the Heisenberg model,[26,33–35] but one notes differences for a small range of small momenta $\mathbf{q}\to\mathbf{0}$. There, the linewidths of our formula (30b) turn out to be too large:

$$\Gamma_{\mathbf{q}}^2 \overset{\mathbf{q}\to\mathbf{0}}{\sim} \mathbf{q}^2;$$

other authors[33] propose at least a dependence $\Gamma_{\mathbf{q}} \overset{\mathbf{q}\to\mathbf{0}}{\sim} \mathbf{q}^2$; This discrepancy must be classified as a consequence of our approximations. Furthermore, our results give $\Gamma_X(T)\sim T^{1.4}$, while the authors of Refs. 33 and 34 suggest a stronger dependence $\Gamma_{\mathbf{q}}\sim T^3$.

TABLE I. Setting of the main parameters used in the calculations for Sec. IV.

Lattice structure	Simple cubic (sc)
Spin value S	$\frac{3}{2}$
Magnon spectral density $S_{\mathbf{q}}(E)$	Gaussian (20)
Conduction band	s band, bandwidth $W=1$ eV, tight binding

IV. KONDO LATTICE MODEL

In order to circumvent the problem of too many possible parameter combinations to discuss, we have chosen three exemplary regions. Small band occupations should be a suitable criterion for ferromagnetic semiconductors and $J=W$ for manganites, where W is the electronic bandwidth. Intermediate J and intermediate n define a parameter range with obvious anomalous magnon softening and damping. The setting of the main parameters is listed in Table I.

Equations (33), (30a), and (30b), respectively, predict that the A_i vanish and, consequently, $\Gamma_{\mathbf{q}}\to 0$ for $T\to 0$K when no magnon-magnon interaction is present. This contradicts the results of other theories of the Kondo lattice model, which give finite linewidths at $T=0$K due to direct contributions to $\Gamma_{\mathbf{q}}$ by electron-magnon interactions.[36,37]

A. Small band occupation

This limiting case is implemented in our calculations by setting $n=0.01$. For all values of $J>0$, the exchange integrals J_{ij} are positive, making ferromagnetism possible (Fig. 2). The growth of the exchange integrals J_{ij} for increasing J is accompanied by a corresponding growth of both the magnon energies $\hbar\Omega_{\mathbf{q}}$ and the linewidths $\Gamma_{\mathbf{q}}$ (Fig. 3). For small J, we find that $\hbar\Omega_{\mathbf{q}}$ and $\Gamma_{\mathbf{q}}$ are nearly independent on the momentum $\mathbf{q}$ since all exchange integrals J_{ij} are of the same order of magnitude. That is why higher exchange integrals $J_{n>1}$ have great influence on $\hbar\Omega_{\mathbf{q}}$ and $\Gamma_{\mathbf{q}}$. However, for $J\approx W$, the magnon energy and linewidth are mainly governed by the nearest-neighbor coupling J_1, and higher exchange integrals can be neglected. Accordingly, $\hbar\Omega_{\mathbf{q}}$ and $\Gamma_{\mathbf{q}}$ converge to the common curve shape of a ferromagnetic nearest-neighbors Heisenberg model.

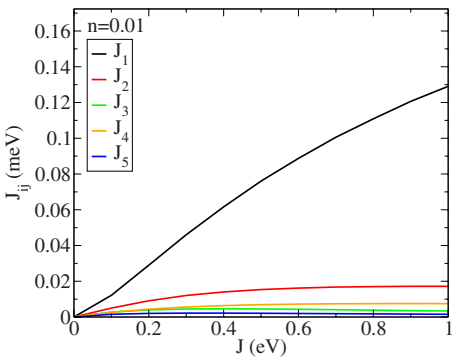

FIG. 2. (Color online) Small band occupation $n=0.01$. Exchange integrals J_{ij} of the first five shells at $T=0.1$ K as a function of the coupling constant J.

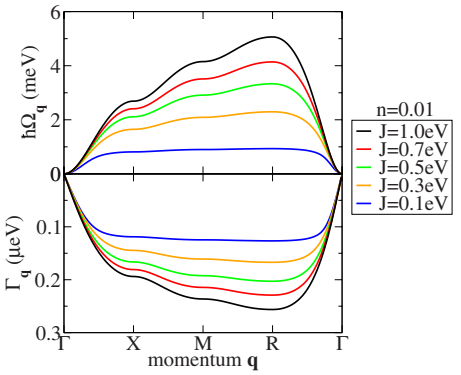

FIG. 3. (Color online) Small band occupation $n=0.01$. Magnon dispersion relation $\hbar\Omega_{\mathbf{q}}$ and momentum dependence of the linewidths $\Gamma_{\mathbf{q}}$ for $T=0.1$K and different values of the coupling constant J.

The spin-resolved electron density of states $\rho_\sigma^{\mathrm{el}}(E)$ (Fig. 4) features the typical properties of the ISA for the case of low temperatures.[18] For weak couplings $J\approx 0$, there is just a small exchange splitting between $\rho_\uparrow^{\mathrm{el}}(E)$ and $\rho_\downarrow^{\mathrm{el}}(E)$. For strong couplings, the $\rho_\downarrow^{\mathrm{el}}(E)$ band splits into two subbands. One is shifted by about $+\frac{J}{2}(S+1)$ to larger energies and is built up by electrons that stabilize their state by permanently absorbing and emitting magnons ("magnetic polaron"). The second band at smaller energies is the scattering band for electrons that have flipped their spin by emitting a magnon. At nonzero temperatures, a high-energy subband for $\uparrow$ electrons too emerges, mainly provoked by thermally excited magnons.

B. "Strong-coupling" regime

Although the strong-coupling regime is often identified with the condition $J \gg W$, we will use this term for the situation $J=W$ as well since it marks a threshold in J where no qualitative deviations appear any more in the quantities which we regard here.

Starting at small band occupations n and with increasing n, the magnon energies $\hbar\Omega_{\mathbf{q}}$ grow and the linewidths $\Gamma_{\mathbf{q}}$ decline (mainly at the X point, Fig. 5). This is made clear by the fact that the exchange integrals J_{ij} first grow because

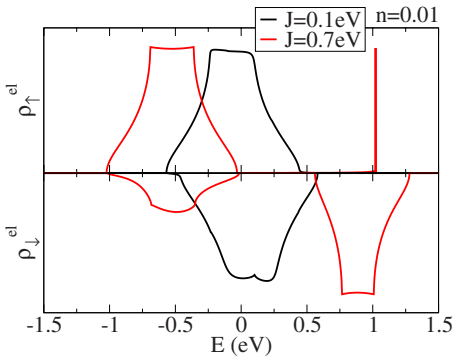

FIG. 4. (Color online) Small band occupation $n=0.01$. Spin-resolved local electron density of states $\rho_\sigma^{\mathrm{el}}(E)$ for $T=5$K and different values of the coupling constant J.

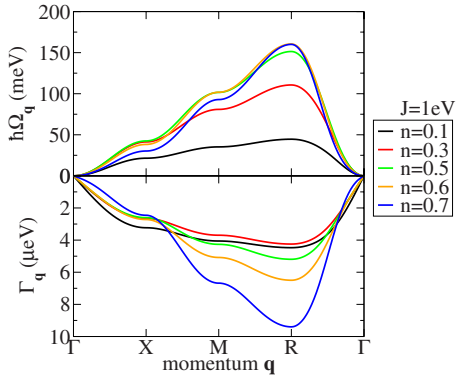

FIG. 5. (Color online) Strong-coupling regime $J=1.0$ eV. Magnon dispersion relation $\hbar\Omega_{\mathbf{q}}$ and momentum dependence of the linewidths $\Gamma_{\mathbf{q}}$ for $T=1$K and different values of the band occupation n.

more indirect exchange between the localized spins is possible when there are more conduction-band electrons present (Fig. 6). $\hbar\Omega_{\mathbf{q}}$ and $\Gamma_{\mathbf{q}}$ reach a maximum (minimum) at about quarter band filling $n\approx 0.5$ and take the usual curve shape of a ferromagnetic nearest-neighbors Heisenberg model. When reaching even larger electron densities n, this behavior is reversed. The energies decrease and the linewidths increase (mainly at the R point), relying on negative higher exchange integrals $J_{n>1}<0$ (antiferromagnetic coupling) and the declining nearest-neighbor coupling J_1. For band occupations above a critical value of $n\approx 0.8$, this trend leads to negative magnon energies that destabilize the ferromagnetic order and prefer antiferromagnetism. The reason why the antiferromagnetic state is more favorable for the case of half band filling $n=1$ can be understood with Pauli's exclusion principle. The electrons can reduce their energy when they virtually hop to adjacent lattice sites, which is only possible if there is no electron with the same spin present.

A study of the temperature dependence (inset of Fig. 6) reveals that primarily the nearest-neighbor coupling J_1 is enhanced for rising temperatures, while higher exchange integrals remain temperature independent.

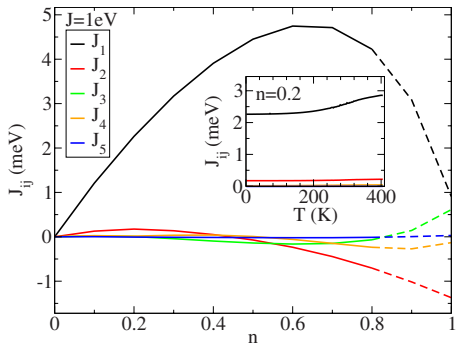

FIG. 6. (Color online) Strong-coupling regime $J=1.0$ eV. Exchange integrals J_{ij} of the first five shells for $T=1$ K as a function of the band occupation n. The broken lines show the behavior according to Eq. (12a) with the setting $\langle S^z\rangle = S$ for values of n, where ferromagnetism is impossible at $T=1$K. The inset shows the temperature dependence of the exchange integrals $J_{ij}(T)$ of the first five shells for $n=0.2$ and temperatures up to T_C.

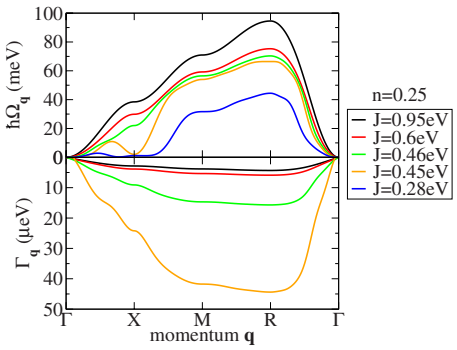

FIG. 7. (Color online) Band occupation $n=0.25$. Magnon dispersion relation $\hbar\Omega_{\mathbf{q}}$ and momentum dependence of the linewidths $\Gamma_{\mathbf{q}}$ for $T=1$K and different values of the coupling constant J. For couplings below $J=0.45$ eV, the equation for $\Gamma_{\mathbf{q}}$ [Eq. (30b)] yields no real solution at $T=1$K, indicating strong antiferromagnetic tendencies in the exchange integrals J_{ij}.

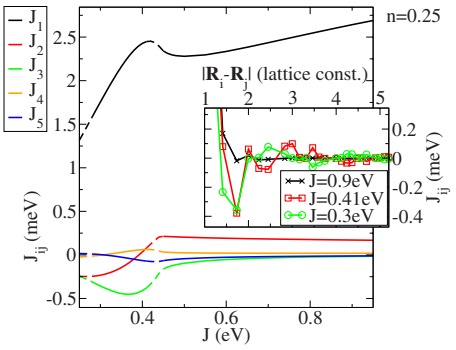

FIG. 8. (Color online) Band occupation $n=0.25$. Exchange integrals J_{ij} of the first five shells for $T=1$K as a function of the coupling constant J. The broken lines show the behavior according to Eq. (12a) with the setting $\langle S^z\rangle=S$ for values of J, where ferromagnetism is impossible at $T=1$K. The inset shows the dependence on the distance $|\mathbf{R}_i-\mathbf{R}_j|$ of the exchange integrals J_{ij} for $T=1$K and different values of J. The lines are guide for the eyes.

C. Anomalous magnon softening and damping

In the case of intermediate couplings J and intermediate band occupations n, the magnon energies and linewidths sensitively depend on both J and n. We investigate the situation for different values of J in the vicinity of a band filling of $n=0.25$ and $J=0.4$ eV.

Higher exchange integrals $J_{n>1}$ are comparatively large and often negative for $J\lesssim 0.5$ eV (Fig. 8), giving rise to distinct deformations of the magnon dispersion relation $\hbar\Omega_{\mathbf{q}}$ and of the curve shape of $\Gamma_{\mathbf{q}}$ mainly at the Brillouin-zone boundaries (Fig. 7). The strongest modifications of the magnon dispersion relation occur around the X point along with smaller ones at the R point. Below a critical $J=0.28$ eV, parts of the Brillouin zone evolve, where the magnon energy becomes negative and for this reason ferromagnetism unstable. The linewidths exhibit deviations from the common behavior of a ferromagnetic nearest-neighbors Heisenberg model between Γ and X point and at the M point. Compared to X and M point, they are unusually small at the R point, which leads to unusually long magnon lifetimes. When approaching the critical J, the linewidths dramatically increase as expected from a Heisenberg model near the transition from the ferromagnetic to the paramagnetic state.

Furthermore, we find distinct long-range oscillations of the exchange integrals between ferromagnetic $J_{ij}>0$ and antiferromagnetic couplings $J_{ij}<0$ qualitatively similar to the conventional RKKY theory (inset of Fig. 8).

It should be pointed out that all the mentioned effects are consequences of solely electron-magnon and magnon-magnon interactions.

When we increase the temperature (Fig. 9), $\hbar\Omega_{\mathbf{q}}$ and $\Gamma_{\mathbf{q}}$ reveal unexpected characteristics. The deviations at the X point in relation to the usual Heisenberg model are reduced, and the magnon energies grow with increasing T — even at temperatures near T_C. This behavior radically differs from the usual behavior observed for a Heisenberg model (e.g., Fig. 1). It relies on the growth of the corresponding exchange integrals $J_{ij}(T)$, mainly of J_1 and J_4, favoring the ferromagnetic order. Furthermore and in contrast to Secs. IV A and IV B and to the results for EuO in Sec. III B, we observe a relatively strong temperature dependence of the linewidths, which behave like $\Gamma_X(T)\sim T^2$ for $J=0.4$ eV (Fig. 9).

Although the magnon density of states (inset of Fig. 9) contains the characteristic tight-binding curve shape, owing to a dominating nearest-neighbor exchange J_1, it exhibits deviations at energies $E\approx 30$ meV and low temperatures due to the deformations in $\hbar\Omega_{\mathbf{q}}$ and $\Gamma_{\mathbf{q}}$. The rise in temperature first leads to larger spectral weight at $E\approx 30$ meV and finally washes out the structure because of the larger linewidths near T_C.

Anomalous magnon softening and damping can be detected in neutron-scattering experiments with manganites.[6–9,38] From the theoretical point of view, anomalous softening at the X point has been reported by other authors,[11,39] confirming the parameter range of intermediate J and n. A theory that features anomalous magnon damping has been proposed by Pandey *et al.*[36] Therein, the spin operators $\mathbf{S}_i$ in the Hamiltonian of the Kondo lattice model (1a) are fermionized by localized electrons in atom orbitals. An "inverse-degeneracy expansion approach" is applied, de-

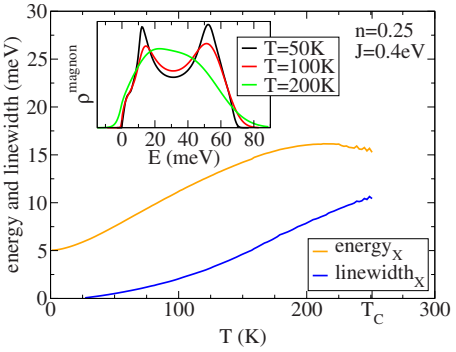

FIG. 9. (Color online) Band occupation $n=0.25$. Temperature dependence of the magnon energy $\hbar\Omega_X(T)$ and the linewidths $\Gamma_X(T)$ at the X point for $J=0.4$ eV. For temperatures below $T=27$ K, the equation for $\Gamma_{\mathbf{q}}$ [Eq. (30b)] yields no real solution, indicating strong antiferromagnetic tendencies in the exchange integrals J_{ij}. The inset shows the magnon density of states $\rho^{\text{magnon}}(E)$ for $J=0.4$ eV at different temperatures up to T_C.

scribing the diagrammatic contributions in powers of the inverse number of orbitals incorporated in the calculations. The authors have mentioned clear differences from the common behavior of a Heisenberg model for $\hbar\Omega_{\mathbf{q}}$ at X and M point and for $\Gamma_{\mathbf{q}}$ between M and R point, even for large $J=6W$ and $J\to\infty$. In the double exchange limit $J\to\infty$, other authors[37] have found anomalous softening and damping too.

V. CONCLUSIONS

We have presented an approach for calculating the magnon energies $\hbar\Omega_{\mathbf{q}}$ and linewidths $\Gamma_{\mathbf{q}}$ for the Kondo lattice model and examined their dependencies on the band occupation n, the coupling constant J, and the temperature T. Likewise, our ansatz allows us to study other interesting quantities such as the electron and magnon density of states $\rho(E)$ or the exchange integrals J_{ij}. We have studied it for small band occupation, the case of $J=W$, and for intermediate J and n, where the magnon spectrum shows anomalies at the Brillouin-zone boundaries. These deviations can be explained by partial antiferromagnetic indirect exchange between the localized spins as a consequence of electron-magnon and magnon-magnon interaction. We have demonstrated that the deformations of the magnon dispersion relation due to anomalous softening become smaller as the temperature rises. As mentioned above, these anomalies are caused by electron-magnon and magnon-magnon interactions only. This finding could permit a better understanding of the origin of similar anomalies in real materials.

Note that our method is also applicable directly to a pure Heisenberg model with given exchange integrals J_{ij}.

When comparing our numerical results with experimental data of $La_{0.7}Ca_{0.3}MnO_3$,[7,9,38] we state differences in $\hbar\Omega_{\mathbf{q}}$ and $\Gamma_{\mathbf{q}}$. Although it is difficult to compare theory and experiment without knowledge of the electronic band structure, it can be argued that the differences can be ascribed to the Hamiltonian (1a), which we have used to derive our results (30a) and (30b). Namely, it does not involve electron-electron, spin-spin, or electron-phonon interactions, even though they are regarded as essential for the manganites. The linewidths calculated by our method turn out to be too small,[7,37] which can be explained by the absent electron-phonon interaction. Moreover, it has been shown that the incorporation of an on-site interaction U between the itinerant electrons changes the magnon dispersion relation drastically.[40] In order to take these terms into account, our approach can be extended.[12,41]

ACKNOWLEDGMENT

This work was supported by the SFB 668 of the "Deutsche Forschungsgesellschaft."

*andrej.schwabe@physik.uni-hamburg.de

[1] W. Nolting, Phys. Status Solidi B **96**, 11 (1979).
[2] M. A. Ruderman and C. Kittel, Phys. Rev. **96**, 99 (1954).
[3] T. Kasuya, Prog. Theor. Phys. **16**, 45 (1956).
[4] K. Yosida, Phys. Rev. **106**, 893 (1957).
[5] N. Furukawa, J. Phys. Soc. Jpn. **65**, 1174 (1996).
[6] J. Zhang, F. Ye, H. Sha, P. Dai, J. A. Fernandez-Baca, and E. W. Plummer, J. Phys.: Condens. Matter **19**, 315204 (2007).
[7] P. Dai, H. Y. Hwang, J. Zhang, J. A. Fernandez-Baca, S.-W. Cheong, C. Kloc, Y. Tomioka, and Y. Tokura, Phys. Rev. B **61**, 9553 (2000).
[8] F. Ye, P. Dai, J. A. Fernandez-Baca, H. Sha, J. W. Lynn, H. Kawano-Furukawa, Y. Tomioka, Y. Tokura, and J. Zhang, Phys. Rev. Lett. **96**, 047204 (2006).
[9] F. Moussa *et al.*, Phys. Rev. B **76**, 064403 (2007).
[10] F. Mancini, N. B. Perkins, and N. M. Plakida, Phys. Lett. A **284**, 286 (2001).
[11] C. Santos and W. Nolting, Phys. Rev. B **65**, 144419 (2002).
[12] M. Stier and W. Nolting, Phys. Rev. B **75**, 144409 (2007).
[13] W. Nolting, S. Rex, and S. M. Jaya, J. Phys.: Condens. Matter **9**, 1301 (1997).
[14] N. Sandschneider and W. Nolting, Phys. Rev. B **76**, 115315 (2007).
[15] M. Kreissl and W. Nolting, Phys. Rev. B **72**, 245117 (2005).
[16] S. Henning (private communication).
[17] We use the identity $\varepsilon_{\mathbf{q}}=\varepsilon_{-\mathbf{q}}$ that is valid for the cubic lattices.
[18] W. Nolting, G. G. Reddy, A. Ramakanth, and D. Meyer, Phys. Rev. B **64**, 155109 (2001).
[19] F. J. Dyson, Phys. Rev. **102**, 1217 (1956).
[20] F. J. Dyson, Phys. Rev. **102**, 1230 (1956).
[21] S. V. Maleev, Zh. Eksp. Teor. Fiz. **33**, 1010 (1957) [Sov. Phys. JETP **6**, 776 (1956)].
[22] T. Holstein and H. Primakoff, Phys. Rev. **58**, 1098 (1940).
[23] V. G. Bar'yakhtar, V. N. Krivoruchko, and D. A. Yablonskii, Theor. Math. Phys. **53**, 1047 (1982).
[24] The restriction to a symmetric spectral density $S_{\mathbf{q}}(\hbar\Omega_{\mathbf{q}}+E)=S_{\mathbf{q}}(\hbar\Omega_{\mathbf{q}}-E)$ facilitates the transition from the spectral moments $M_{\mathbf{q}}$ to $\hbar\Omega_{\mathbf{q}}$ and $\Gamma_{\mathbf{q}}$. The corresponding substitution in the integral in Eq. (15) is $\frac{E-\hbar\Omega_{\mathbf{q}}}{\Gamma_{\mathbf{q}}}\to E$.
[25] O. W. Dietrich, J. Als-Nielsen, and L. Passell, Phys. Rev. B **14**, 4923 (1976).
[26] R. A. Tahir-Kheli and D. Ter Haar, Phys. Rev. **127**, 95 (1962).
[27] The lattice sites can be ordered by any other pattern as well. Anyhow, for an isotropic magnetic system with $J_{ij}=J_{ij}(|\mathbf{R}_i-\mathbf{R}_j|)$, it seems natural to require $|\mathbf{R}-\tilde{\mathbf{R}}|=$const for a shell.
[28] We use the identity $\gamma_{\mathbf{q}}=\gamma_{-\mathbf{q}}$ that is valid for the cubic lattices.
[29] H. Dvey-Aharon and M. Fibich, Phys. Rev. B **18**, 3491 (1978).
[30] L. Passell, O. W. Dietrich, and J. Als-Nielsen, Phys. Rev. B **14**, 4897 (1976).
[31] J. Als-Nielsen, O. W. Dietrich, and L. Passell, Phys. Rev. B **14**, 4908 (1976).
[32] C. J. Glinka, V. J. Minkiewicz, L. Passell, and M. W. Shafer, AIP Conf. Proc. **18**, 1060 (1974).
[33] J. F. Cooke and H. A. Gersch, Phys. Rev. **153**, 641 (1967).
[34] W. Marshall and G. Murray, J. Appl. Phys. **39**, 380 (1968).
[35] A. B. Harris, Phys. Rev. **175**, 674 (1968).
[36] S. Pandey, S. Das, B. Kamble, S. Ghosh, D. Singh, R. Ray, and A. Singh, Phys. Rev. B **77**, 134447 (2008).

[37] D. I. Golosov, Phys. Rev. Lett. **84**, 3974 (2000).
[38] F. Ye, P. Dai, J. A. Fernandez-Baca, D. T. Adroja, T. G. Perring, Y. Tomioka, and Y. Tokura, Phys. Rev. B **75**, 144408 (2007).
[39] M. Vogt, C. Santos, and W. Nolting, Phys. Status Solidi B **223**, 679 (2001).
[40] M. D. Kapetanakis and I. E. Perakis, Phys. Rev. B **75**, 140401(R) (2007).
[41] W. Nolting *et al.*, Phys. Rev. B **67**, 024426 (2003).